Energy Engineering

Tech Science Press

Doi:10.32604/ee.2025.061617

ARTICLE

Nanoparticle Distribution in Compression Ignition Engines Using Rapeseed Methyl Ester

Hayder A. Dhahad[1], Miqdam T. Chaichan[2,*], Mohammed A. Fayad[2], Hasanain A. Abdul Wahhab[3] and T. Magrites[4]

[1]Mechanical Engineering Department, University of Technology-Iraq, Baghdad, 10001, Iraq
[2]Energy and Renewable Energies Technology Centre, University of Technology-Iraq, Baghdad, 10001, Iraq
[3]Training and Workshop Center, University of Technology-Iraq, Baghdad, 10001, Iraq
[4]Centre for Advanced Powertrain and Fuels Research School of Engineering and Design, Brunel University, London, UB 83PH, UK

*Corresponding Author: Miqdam T. Chaichan. Email: miqdam.t.chaichan@uotechnology.edu.iq

Received: 28 November 2024; Accepted: 13 January 2025; Published: 31 March 2025

ABSTRACT: One of the most important of these emissions is fine particulate matter, which is a harmful emission of diesel engines, leading to the imposition of strict regulations. Biodiesel, with its high oxygen content, is an effective alternative to significantly reduce these emissions. In this study, rapeseed methyl ester (RME) was used as a diesel engine fuel and the emitted particulate matter was compared with ultra-low sulfur diesel (ULSD). In most experimental studies, the emission of soot was measured. In this work, the effects of injection timing, injection pressure (IP), and engine load on fine particulate matter in both nucleation and accumulation modes were studied. The results show that IP increases the number of particles in the accumulation mode while the number of particles in the crystallization mode is higher for rapeseed methyl ester (RME) than for ultra-low sulfur diesel (ULSD). Conversely, the formation rates of particles in the accumulation mode are higher for ULSD. Cumulative concentration numbers (CCN) are generally higher for RME in crystallization mode but higher for ULSD in accumulation mode. Increasing the IP reduces the CCN values. The particle size in crystallization mode reaches a maximum of 22 nm at IPs of 800 and 1000 bar but decreases to 15 nm at 1200 bar. Most fine particles fall in the 5–100 nm diameter range. High engine loads reduce the particle size distribution in nucleation mode for both fuels, with a slight increase in particle size in nucleation mode. The study concluded that the use of rapeseed methyl ester as an engine fuel benefits the environment and improves air quality due to the significant reduction in the size, number, and concentration of nano-soot particles and total particles emitted from the engine.

KEYWORDS: Injection pressure; injection timing; nucleation and accumulation; particulate matter; premixed burn; smoke number

1 Introduction

The growing global population and improving living standards have significantly increased the number of vehicles reliant on fossil fuels, gives challenges to achieving net-zero emissions and the United Nations Sustainable Development Goals (SDGs). Addressing these challenges requires transformative changes in social and economic systems, alongside a fundamental shift in the global energy landscape [1]. Excessive fossil fuel consumption has severely impacted air quality and exacerbated environmental issues such as climate change and global warming. In addition, diesel engines usually emit only carbon dioxide (CO_2) and water vapor during combustion, real-world conditions result in incomplete combustion, leading to a range of harmful emissions. To meet with global sustainability targets, researchers, designers, and automakers

have introduced substantial advancements in engine design aimed at minimizing emissions and mitigating environmental harm. These efforts are essential to fostering a cleaner, more sustainable future [2].

Of all the emissions from CI engines, fine particulate matter (PM) is certainly one of the most hazardous and has gained increasing attention as measurement techniques have improved. Diesel engines are significant sources of PM because when they burn fuel, 0.2 to 0.5 percent of the mass is converted into fine particulate matter consisting of particles of 1 nm to 0.1 μm in size [3]. Such particles, when first dispersed in the air, pose a risk to human and animal life, as demonstrated by mechanical and medical analysis. The composition of PM mainly includes liquid H_2SO_4 and organic species that have high volatility and condense during dilution and cooling to form nanoparticles [4].

PM emissions include three main components: sulfate particles, soluble organic compounds, and carbonaceous sorbents, or soot in general. Soot is produced chemically and physically, when large aromatic hydrocarbons stick together and mix with carbon nuclei to form spherical or semi-spherical, round or irregular masses. These particles are developed during the thermal decomposition of fuel in an engine, known as partial combustion, where temperature and oxygen conditions favor the cleavage of the hydrocarbon chain [5].

Soot emissions are detrimental to health because as a pollutant they contribute to diseases such as lung cancer, respiratory diseases, and cardiovascular diseases. Current research shows that these emissions are dangerous because they aggravate allergic diseases and affect major organs of the body. The formation of fine particles occurs in two stages: the nucleation mode (Nuc). The first is the nucleation mode (>60 nm), where either carbon or sulfur nuclei of nano-sized size are formed and the second is the accumulation mode, where these nuclei grow and coagulate. The main parameters that regulate the size and number of fine particles are injection pressure (IP), load, and injection timing (IT). The effect of these variables on the particle number concentration and size distribution will be presented in the following sections [6].

Conditions such as chronic lung diseases, lung cancer and asthma, which are major causes of high mortality, are associated with concentrations of particulate matter, especially PM10, PM2.5 and PM1. These fine particles reach the lungs, clog the capillaries and cause severe health effects [7].

Biodiesel, which is produced from vegetable oils or animal fats by the process of transesterification, consists of a mixture of monoalkyl esters of fatty acids and glycerol. It is renewable and emits low level of hydrocarbons (HC), carbon monoxide (CO) and PM than conventional fossil diesel. Unleaded biodiesel and biodiesel blends (B 100, B-20 and B-50, respectively) were environmentally friendly with minor changes in nitrogen oxide (NOx). For example, EPA Tier II engines are further investigating CO_2, HC, ethylene and PAHs, which are reduced by 25% in a biodiesel blend, B25, at high loads but increase NOx [8].

Scientists have made biodiesel from a variety of feedstocks including cottonseed oil, waste oil, fish oil and palm oil [9–11]. Although biodiesel boosts emissions, its combustion characteristics are not constant, depending on the feedstock and blend level [12–15]. Compared to Diesel, exhaust emissions from pure biodiesel slightly increase fuel economy and NOx while significantly eliminating hydrocarbon, carbon monoxide and particulate emissions [16–19].

Modern investigations have also shown that the presence of nanoparticles, such as cerium dioxide, in biodiesel blends results in better combustion properties and a 45.59% reduction in hydrocarbons and carbon dioxide and 32.16% in carbon dioxide, accompanied by a very small increase in nitrogen oxides. The incorporation of cerium dioxide also reduces the emission of polycyclic aromatic hydrocarbons (PAH) and soot [20]. In another example, biodiesel from fish oil in its pure and blended form has been shown to reduce soot and particulate emissions by 70%–90%, proving that higher oxygen content improves fuel oxidation.

The literature review on biodiesel also includes studies on injector nozzle design with a focus on emissions and IP along with IT, leading to improved engine performance from biodiesel and other fuel options [21–25].

After a critical evaluation of the literature, it was found that very little literature has focused entirely on exploring the emissions from diesel engines during the combustion phase, especially soot. Although there have been several attempts to study the performance of several types of diesel engines operating on various types of biofuels or their blends with diesel and the effect of the main operating conditions on the emitted pollutants. Due to this lack of information, experiments were conducted to measure the particulate matter emissions under ultra-low sulfur diesel (ULSD) and RME operating scenarios inside the engine. This experimental work aims to reveal the relationship between the combustion phase and the PM emissions and covers the examination of changes in injection timing (IT), injection pressure (IP) and engine load as well. From previous and recent studies, it was noticed that there are few studies that have measured the particulate matter emissions during operating conditions, using current injection systems such as the high-pressure injection system (HPIS), as in the present study. Such measurements would further expand this research area. Current experimental attempts address the complex effects of injection techniques that include injection strategies as well as procedure characteristics (IT, injection rate, IP, and injection strategies) targeted for PM generation emitted from both the accumulation mode (Acc.) and nucleation mode (Nuc.). The following important influence on the effectiveness of these strategies is analyzed in the section on PM sources and distribution, with emphasis on concentration and size distribution.

2 Materials and Methods

2.1 Fuel Properties

Two fuels have been used in the current study: Rapeseed Methyl Ester (RME) and Ultra Low Sulfur Diesel (ULSD). Shell Global Solutions provided the RME fuel. This fuel is used in petrol stations in the United Kingdom and is approved for use by the authorities there due to its proven good performance and low exhaust emissions compared to diesel. ULSD was purchased from local fuel stations in London. The fuels' properties (physical and chemical) are listed in Table 1. Both fuels were used in their neat condition without any mixing. The fuel consumption is controlled by the Electric control unit, which changes the fuel consumption according to engine operation variables such as speed and load.

Table 1: RME and ULSD Fuels specifications [13]

Specification	Measuring unit	Method	Diesel (ULSD)	Biodiesel (RME)
Chemical formula			$C_{14}H_{26.18}$	$C_{18.96}H_{35.29}O_2$
Cetane number	–	ASTM D7668-14	54	54.7
Density at 15°C	(kg/m^3)	EN 12185	827	882.54
Viscosity at 40°C	(cSt)	EN ISO 3104	2.397	3.516
Lower calorific value (LCV)	(MJ/kg)		43.29	37.39
Sulphur	(mg/kg)		7	2
Aromatics	(wt%)		25	00
Carbon	(wt%)		87	76
H_2	(wt%)		14	13
O_2	(wt%)		00	11
Cloud point	°C		−9	−18

(Continued)

Table 1 (continued)

Specification	Measuring unit	Method	Diesel (ULSD)	Biodiesel (RME)
Flash point	°C		67	72
Ash content	(wt%)		<0.005	<0.005

2.2 Test Rig and Accessories

The schematic diagram illustrated in Fig. 1 represents the rig used in the experiments. Ford Motor Company makes the diesel engine used in the tests. The engine name is Puma engine, which is a direct injection high-speed diesel engine. Each cylinder has four valves and is powered by twin camshafts. The intake manifold with a straight cylinder feed, 2.0 L capacity, and 18.2:1 compression ratio (CR) is fitted with a Garrett turbocharger. This engine is equipped with a Schenk Eddy dynamometer attached to the motor. The dynamometer is used to control the torque subjected to the engine. The engine settings were controlled by engine map writing and modification computer running GrEDI v 2.298.

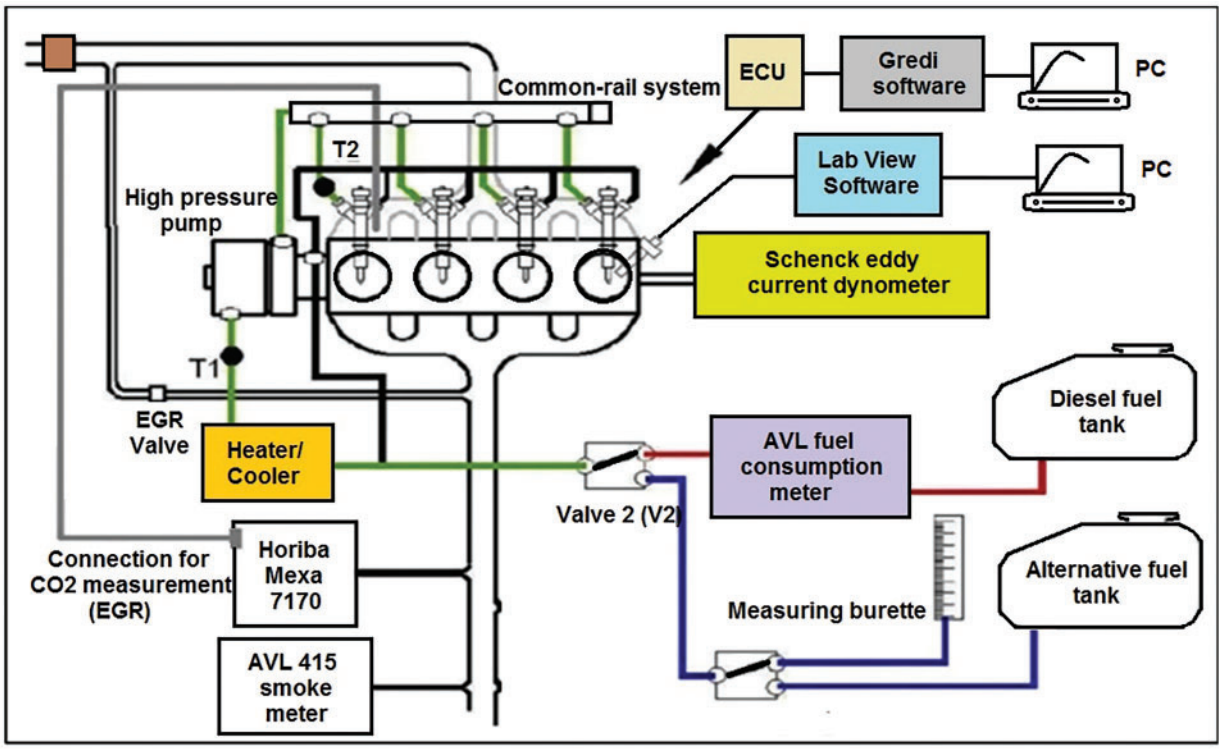

Figure 1: Schematic diagram of the experimental setup

Electronic control unit (ECU) specifications can be directly manipulated using GrEDI software. A number of parameters can be controlled using this software, including injection timing (IT), injection pressure (IP), boost pressure, and exhaust gas recirculation (EGR). The ECU monitors temperatures, pressures, flow rates, and voltages, while GrEDI provides readings of these parameters. Secondary measurements can also be used to verify these values. Engines powered by Puma are equipped with high-pressure injection systems from Delphi Diesel Systems Ltd. (DDS). In addition to being able to work at high IPs such as 1600 bar,

this rod can also operate at low pressures. An injection control unit (ICU) with common-rail fuel injection system was used to regulates fuel injection pump pressure by which the right volume and timing of fuel is injected. Before injectors are opened, ICU inputs like fuel pump temperature, common rail pressure, and engine parameters are determined. The injectors have six holes (0.154 mm diameter) and a spray angle of 154°. It is possible to measure the pressure within cylinder No. 1 by installing a transducer (type Kistler 6125 piezoelectric). For the experiments, Brunel University developed LabVIEW version 6.0 to collect and save cylinder pressure data. A hundred drive cycles were taken for each measurement. Two fuel tanks supply were fed this rig and there was no mixing between the fuels. Each fuel was used as pure state in the test, as illustrated above.

Engine load and speed are controlled by the W130 Schenck Eddy—which uses eddy currents to create a magnetic field that causes the rotor to break. The dynamometer can control engine torque and speed. Exhaust gas samples were obtained through the exhaust manifold pipe. Sample ports are drilled in several places of the tube and provided with the necessary fittings for delivering samples to exhaust gas analyzers.

2.3 Particulate Matter and Smoke Measurements

A smoke meter equipped with an AVL 415S measures filter smoke number (FSN) has been used in the tests. Automatic adjustment of the sample size or effective length is possible with this apparatus. With its accuracy of 0.002 FSN, the device measures smoke numbers from 0 to 10. Zero number represents the white paper filter and shows that the soot concentration is 0 mg/m^3, while the number 10 represents completely black paper, and the soot concentration is then 32,000 mg/m^3. For all practicaluate measurements, three samples were taken, and their average was considered as the result to be analyzed. To obtain the exhaust particle size distribution, electrostatic motion spectrometry (EMS) was used in the experiments. It is designed in three levels: EMS control center software, Internet-based control devices and smart devices. Also, this device was uswd to measure the number and size of particulate in the exhaust pipe for RME and diesel. The spectrometer used is flexible, and the platform can be easily extended with new peripherals. The basic parameters of the measurement system used in the study for measuring PM emissions and distribution are shown in Table 2.

Table 2: Basic parameters of the measurement system used in the study

Parameters	Measurement's system	Using
ICU	Electric control unit	To control the injection strategies
AVL 415S	Smoke meter	To measure the Filter smoke number
EMS	Electrostatic mobility spectrometer	To obtain the exhaust particle size distribution
W130 Schenck Eddy	Current dynameters	To control the engine load and speed
FTIR	Fourier-transform infrared spectroscopy	To measure the exhaust gas emissions

2.4 Data Analysis

Raw data and various measurements were collected using LabView in MATLAB and were stored for later processing and utilization of relevant information. Engine load information and variables such as in-cylinder pressure, start-of-combustion angle (SOC), peak pressure, and peak pressure angle can correlate their effects on smoke and PM measurements.

The cumulative concentration number (CCN) for soot particles can be calculated employing the equation:

$$CCN = \sum_{i=1}^{n} \left[\frac{dN}{dlnD\,(i)} . dlnD(i) \right] \tag{1}$$

where: n—Consecutive particle diameter (number of channels). $\frac{dN}{dlnD(i)}$ stands for Particle concentration number, and $dlnD$ is the width of the size interval for a channel.

2.5 Uncertainty Analysis

By measuring the standard error (SE), inferential statistics determine how closely or fairly the sample data represents for all experiments. Likewise, for standard deviation, which brings an understanding of the dispersion of a single sample with several measurements, SE shows the changes and fluctuation in measurement across multiple samples statistically. Standard deviations from the standard value of the devices become known after calibration. Then, researchers can use these devices in practical experiments. The equipment results shown in Table 3 show the standard error measurements of the devices used and the unreliability rate was low (less than 3%), which means high measurement accuracy. In order to ensure accuracy, the experiment was repeated at least three times and then a geometric mean was calculated.

$$\text{Standard error} = \frac{s}{\sqrt{n}}$$

where:

$$\text{s: } \frac{\sqrt{\sum n_1(x_i - \overline{x})}}{n-1} \tag{2}$$

where: xi: a random variable, $\bar{x}$: sample mean, and n: sample size.

Using standard deviation, the precision of a sample distribution can be measured with a statistical term. In statistical terms, SE represents the deviation from the actual mean.

Table 3: The accuracy and uncertainty of the instruments used in the current study

No.	Engine measurement	Accuracy	Uncertainty (%)
1	Load	±1 N	±0.53
2	Speed	±7 rpm	±0.3
3	Flow meter (fuel)	±0.15 cc	±1.15
4	Thermocouples	±1°C	±1.1
5	Flow meter (Air)	±0.09 bar	±0.6
6	Smoke meter (AVL 415S)	±0.2%	±0.5
7	Electrostatic mobility spectrometer	±0.3%	±0.52
8	Current dynameters	±0.25%	±0.24
9	FTIR	±1.2%	±0.6

Table 4 shows the conditions under which experiments are carried out for the two tested fuels. Further, under all operating conditions, measurements were taken three times, and the curves show the arithmetic mean of these readings. Here, it should be noted that the injection timing −9° ATDC represents the start of the injection, and this value represents the optimum injection timing for the reference fuel (ULSD).

Table 4: The test conditions used in experiments

Variable	Value
Load	2.5, 5
Engine speed (rpm)	1500
Injection pressure (bar)	800, 1000, 1200
Injection timing °ATDC	−9
Dilution ratio	32.5
Dilution gas temperature (°C)	300

3 Results and Discussion

3.1 PM Number Concentration and Size Distribution at Variable IPs

Injection pressure (IP) effects on the particle numbers, size, and distribution of the tested fuels ULSD (Figs. 2 and 3) and RME (Figs. 4 and 5) at low and high engine loads. Most of the particle sizes measured are from 5 to 100 nm in diameter. For ULSD fuels, at low engine loads (2.5 bar), the particle size is reduced to a range of 5 to 40 nm with increasing IP (Fig. 2). This reduction indicates that increasing the IP decreases the particle sizes during nucleation. At IPs of 800 bar and 1000 bar, the peak Nuc. M is at 22 nm while it decreases to 15 nm at the IP of 1200 bar in the Nuc. M, the particles are formed during the dilution process in the exhaust. During this process, a part of the semi-volatile particles in the Nuc. M is condensed on the surface of the Acc. M particles can also volatilize into the nucleated particles as well. The synonymous trends of RME combustion are the evidence as represented in Figs. 4 and 5. For instance, during low engine load conditions, the peak Nuc. M will be the cause of emissions. The COS distance values reached 18 nm for both the IPs 800 bar and 1000 bar, but they dropped to 15 nm with an IP of 1200 bar. On the contrary, when the engine undergoes high loads, it produces a high peak level of Nuc. With an increment of pressure from 800 to 1000 to 1200 bar M was decreased from two nanometer (nm) to one nanometer (nm).

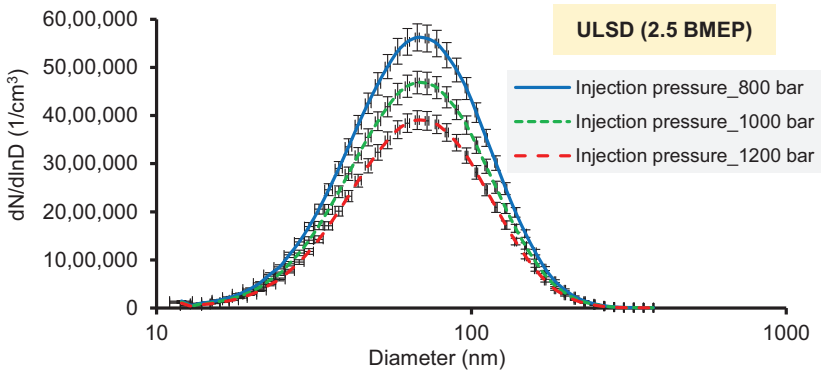

Figure 2: At low engine loads, the effect of IP on ULSD particulate numbers and size distribution

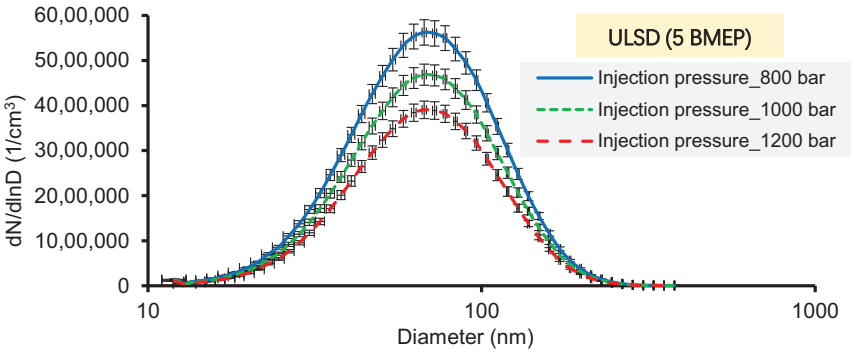

Figure 3: Particulate number concentration and size distributions for ULSD under high engine loads and variable IP conditions

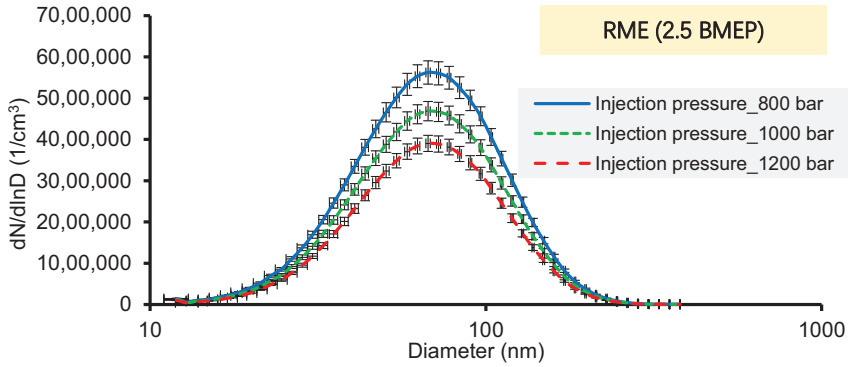

Figure 4: Particulate number concentration and size distribution for RME at low engine loads and IP conditions

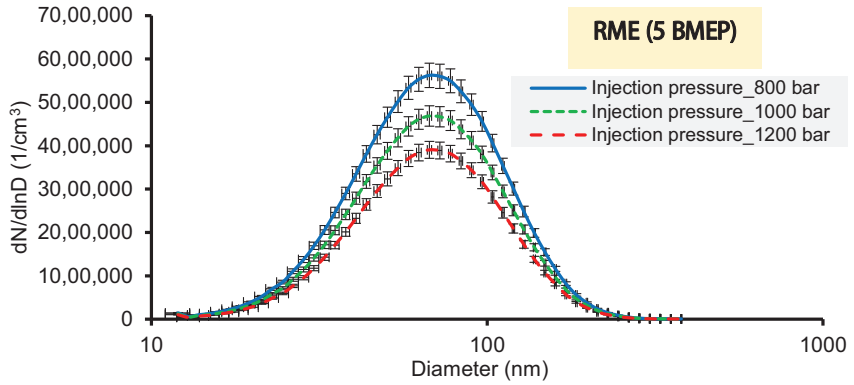

Figure 5: Particulate number concentration and size distribution for RME at high engine loads and variable IP conditions

Magno et al. [26] showed the existence of a reciprocal relationship between particles in the accumulation and Nuc. Ms. Increasing the IP causes better fuel atomization, which enhances the fuel evaporation and mixing with the air process; as a result, the combustion process improves, and the large particles emitted (Acc. M) reduce the emitted soot. The PM in the accretion mode consists of groups or chains of particles that are formed during the fusion and growth of particles (resulting from nuclei of products resulting

from incomplete combustion). Nuclei sizes and concentrations are affected by combustion conditions, coagulation, as well as the levels of aromatic hydrocarbon in the fuel composition [28]. Running the engine at high loads (Fig. 3) makes larger quantities of fuel injected with the same intake air, so the particles formed increase. Increasing the number of particles facilitates the coagulation process and increases its rates, resulting in larger particle diameter formation.

The effect of IP on particles formed in the Acc. M is more pronounced than on the particles formed in the Nuc. M. The number of particles formed in the Acc. M decreases with increasing IP. In this case, the burning rate of the pre-prepared mixture increases with increasing IP, causing a significant reduction in the rate of soot formation by limiting the growth of the nanoparticles and coagulating together to form larger smoke particles. Furthermore, increased IP improves fuel atomization, which results in better fuel evaporation and air mixture. This process leading to an improvement in the combustion quality and reduces the emissions of large particles in the accumulator mode. The result of such a process is a reduced concentration of soot emitted. The PM in the Acc. M consists of formed chains or nuclei that fuse and grow in the zones where rich fuels form and result in an incomplete combustion. The particulates (size and concentration) depend on the oxidation levels, coagulation rates, and the aromatic hydrocarbon content of the fuel.

Figs. 6 and 7 compare the results obtained in the previous figure for both fuels. For RME, the number of smaller nucleation particles is higher than the ULSD condition for all operating conditions of the research engine (Fig. 6), while for ULSD, the Acc. M particulates are higher than the RME state (Fig. 7). The sulfur content of the RME is very low which result in the reduction of nucleation. The absence of aromatic hydrocarbons (which facilitates the dissolution of organic parts) reduces condensation and absorption on the surface of soot particles. Second, RME is characterized by its high viscosity, which causes fuel drops to be slower than to the diesel. Also, it is low rate of mixing with air in multiple (local) zones within the combustion chamber, causing an increased amount of Nuc. M particles generated. RME contains high oxygen levels in its composition, which is an important factor in reducing the size of carbonic particles. Zheng and Cho [27] showed that the operation of a biodiesel combustion engine and its blends with diesel resulted in particulate concentrations in the Nuc. M higher than the engine operating condition with a neat ULSD. They also found that biodiesel and its mixture with diesel produced low particulate concentrations in the Acc. M (especially at high load). The effects of the abundance of oxygen, high viscosity, and the absence of aromatic hydrocarbons interfere with each other and the result is growth in the number of particles formed in the Nuc. M. This result agrees with the results of [28].

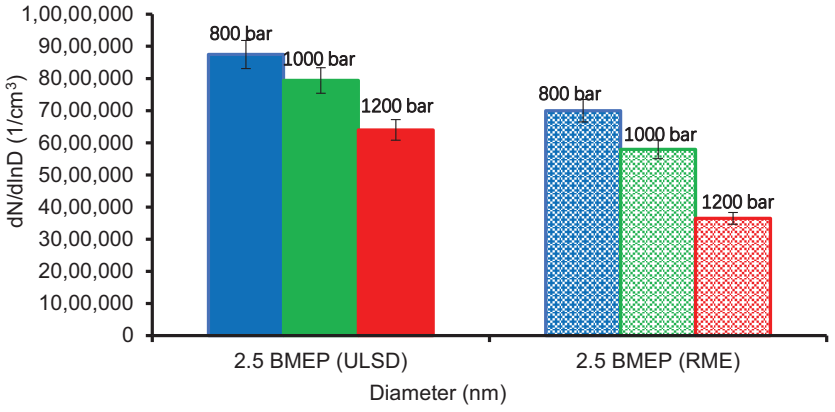

Figure 6: At low loads, the impact of IP on RME and ULSD particulate number concentration and size distribution

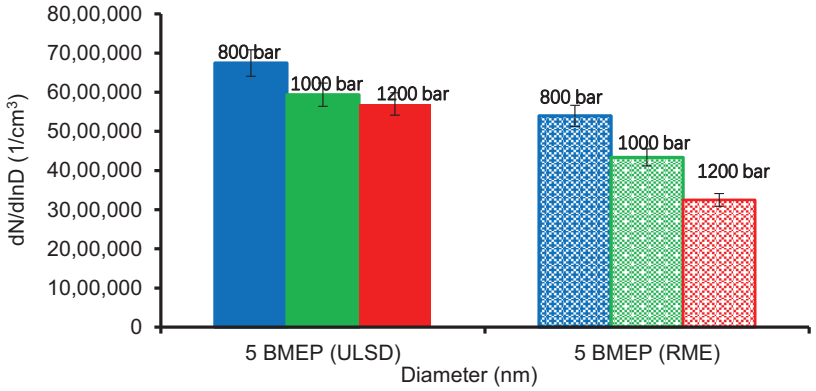

Figure 7: At high loads, the impact of IP on RME and ULSD particulate number concentration and size distribution

Eq. (1) makes it possible to calculate CCN, which facilitates calculating the cumulative number of Nuc. M and accumulation according to particle sizes. In this study, particulates with (dia. < 40 nm) were adopted as Nuc. M emissions and particulates with (dia. > 40 nm) as Acc. M emissions. Figs. 8 and 9 show the relationship between IP and CCN for both nucleation and Acc. M s at different IPs for both types of fuel. Fig. 8 shows that the nucleated CCN values of RME are higher under most conditions, while the accumulation CCN values of ULSD are higher. By increasing the IP, the combustion quality improves, and all CCN values decrease. In general, CCN values at low loads (Fig. 9) are less than their values at high loads, especially at high IPs. This result is due to enhancements in the fuel premixing process at these mixing ratios, which results in a higher premixed combustion rate.

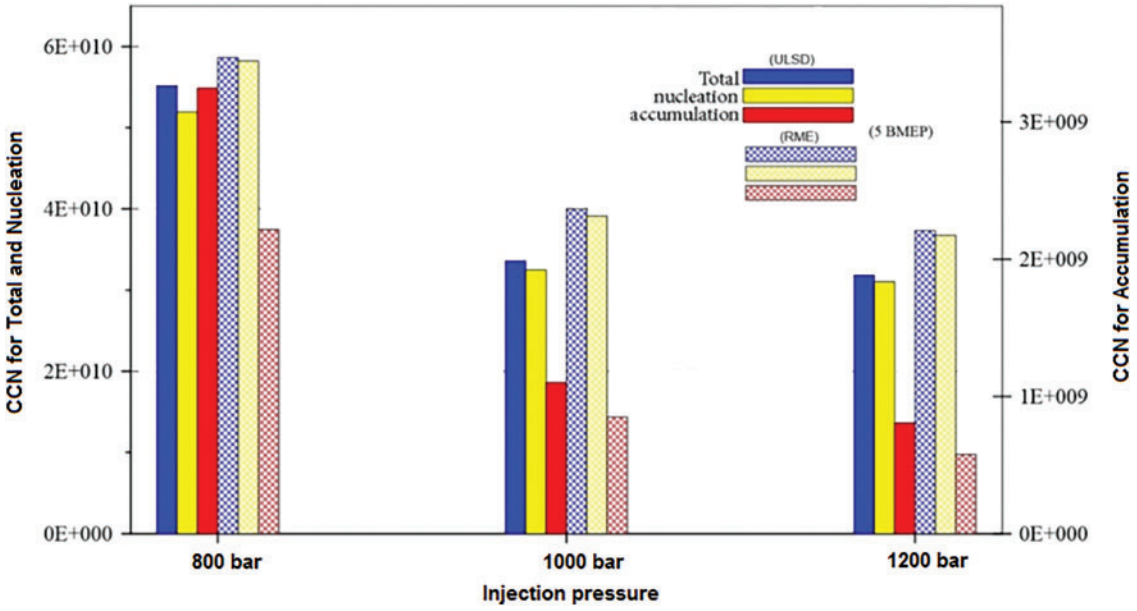

Figure 8: IP effect on CCN for total and Nuc. and Acc. Ms at high load

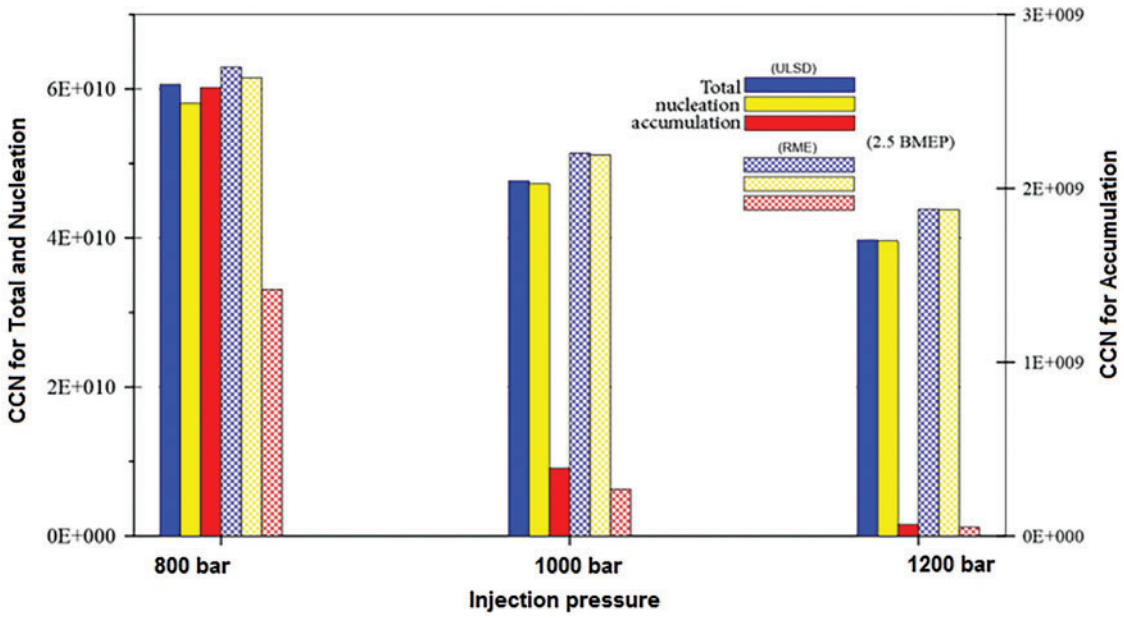

Figure 9: Effect of IP on CCN for total and Nuc. and Acc. M at low load

3.2 Load Effect on Particle Number Concentration and Size Distribution

Figs. 10–12 exhibit the effect of engine load variation on the PM number size distribution for USLD (Fig. 10) and on the RME (Fig. 11). The experiments were conducted at fixed engine speed (1500 rpm), constant IP (800 bar) and constant IT (−9°ATDC). USLD curves show that most of the measured particles are between 5 and 100 nm in diameter. As the load increases, the number of nucleated particles with diameters ($d < 40$ nm) decreases. The peak of the Nuc. M appears at 22 nm. In the accumulator mode, the particle number values for the diameters converge from 40 to 67 nm, and there is a limited increase with increasing motor load. About 75% of the fuel burned is premixed, which reduces nucleation and coagulation to form larger PM. However, at high engine loads, more fuel is burned to ensure a constant speed, causing higher rates of particulate formation. The number of particles formed increases results in increasing the coagulation rate, forming particles of larger diameters and sizes. At high engine loads, the air/fuel ratio reduces by increasing the amount of fuel injected at the expense of excess oxygen. The combustion chamber temperature also increases with increasing engine load, which enhances combustion/re-combustion of particles inside the combustion chamber prior to their exit from the exhaust valve, as a result of which their concentrations were decreased significantly. Srivastava et al. [29] stated that of all engine variables, temperature has the most important influence on particle formation as the combustion chamber temperature increases the rates of reactions related to the formation of soot and its oxidation. Lapuerta et al. [30] indicated that the increase in the oxidation rate is more evident with the increase in combustion chamber temperature compared to the rate of particle formation. Under these conditions, pressure and temperature levels rise, which promotes the growth of new soot nuclei. When the engine is running at low loads, the levels of particles formed in the Nuc. M were decreased as a result of their accumulation. Fig. 11 shows similar behavior when running with RME, the peak Nuc. M is on the order of 18 nm.

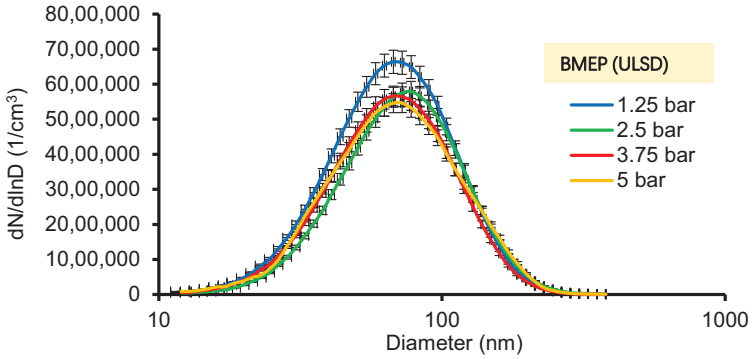

Figure 10: Load variation effect on PM concentration and size distribution for ULSD

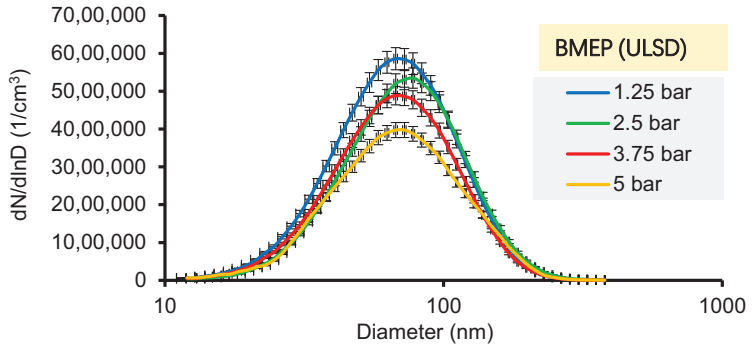

Figure 11: Load variation effect on PM concentration and size distribution for RME

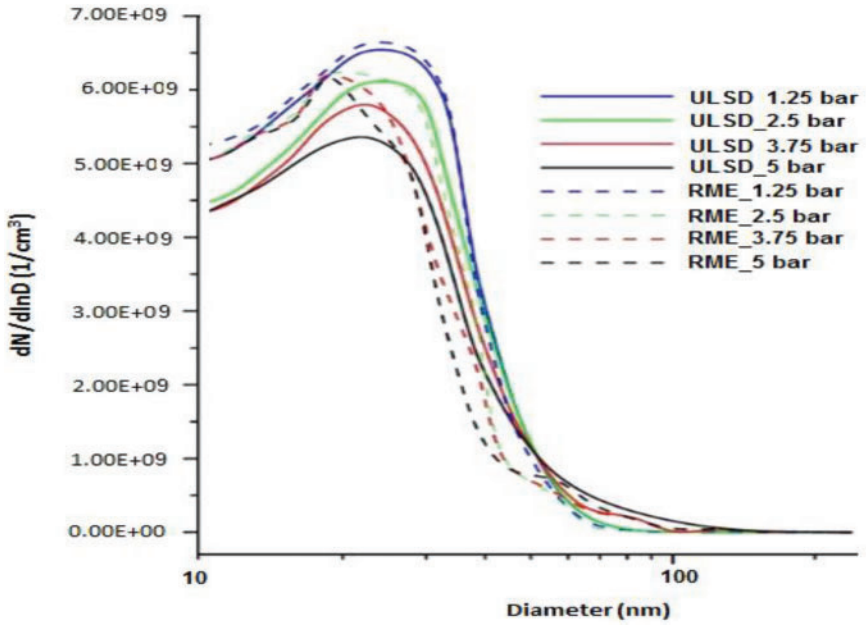

Figure 12: Comparison between the road variation effect of PM concentration and size distribution for ULSD and RME

At medium and high engine loads, the effect of the load on the Nuc. M is limited, as the particle number concentrations are very close. An increase in particulate emissions is observed in the Nuc. M from RME combustion compared to the ULSD combustion in the engine, while these concentrations in the accumulating mode are higher when working with ULSD compared to RME. Schneider et al. [31] investigated the composition and size of PM were studied using mass spectrometry. The study showed that running the engine with ULSD allowed the condensation of low-volatile and semi-volatile hydrocarbons when only the particle accumulator was set to form larger particle-size particles. This result is related to the engine load, at high loads, the exhaust gas temperature rises, which facilitates the increase in the rates of PM formation.

Fig. 13 demonstrates the influence of engine load on CCN in both nucleation (Nuc) and accumulate (Acc) modes through the use of test fuels. As engine loading increases, the effect of nucleated CCN is reduced for both fuels while the mass concentration of CCN goes up. The outside-in coagulation may change around the higher engine loads since the coagulation speed of the particulates is faster at the condition, and larger particle agglomerates will be formed. Apart from that, fewer particles of Acc. M mode accrual comes from RME, and the initial number of above 40 nm particles is minimized. This reduction is due to the properties of RME to displace part of the oxygen contained in HFO as well as several other additives.

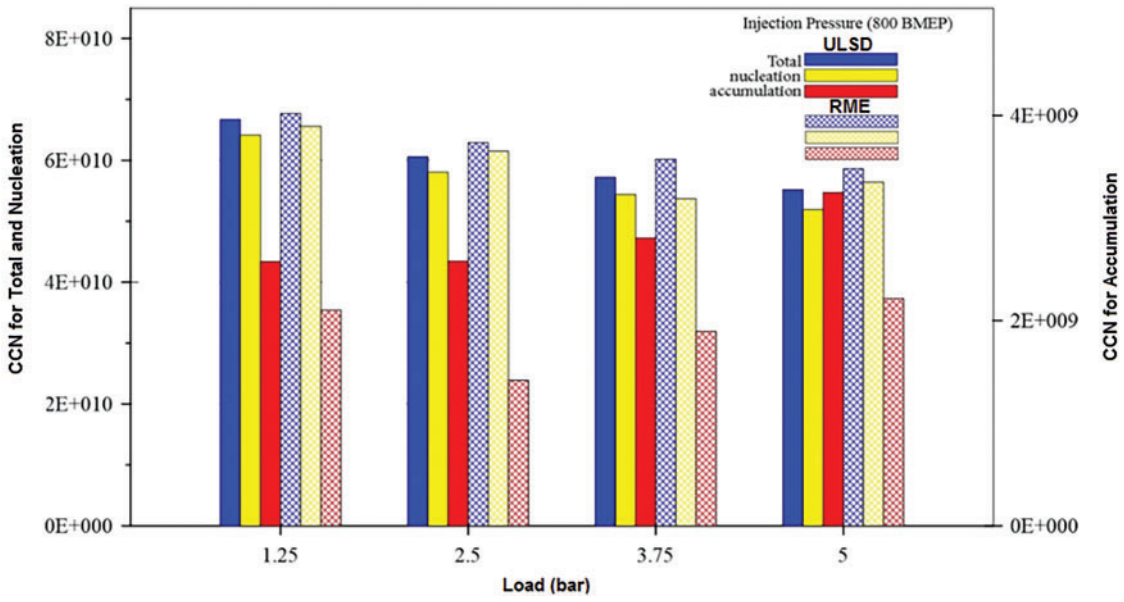

Figure 13: Effect of load on CCN for total and nucleation & Acc. M

4 Conclusions

In this study, the effect of a number of compression ignition engine operational variables (namely IT, IP, and engine load) effects was examined on the particulate size distribution of ULSD and RME fuels. The main conclusions from the current study were summarized as follows:

- Effect of IP variation: IP affects particle count and size with reference to the type of fuel tested and engine loads. It is observed that in the nucleation process at low engine loads, such as 2.5 bar with ULSD fuel and with increasing IP, particle sizes decrease and fall in the range of 5 to 40 nm. The primary peak mode is observed at 22 nm for injection pressures of 800 bar and 1000 bar and decreases to 15 nm for IP of 1200 bar.

- Effect of changing engine load on PM number size distribution: For USLD fuel, with increasing load, the number of particles less than 40 nm in diameter is reduced, and the nucleation mode is at 22 nm, which represents Nuc. M. As for the accumulation mode case, the particle numbers increase in the range from 40 to 67 nm, with a marginal increase as the engine load increases. Higher loads cause the engine to burn more fuel to maintain speed; Thus, more particles are formed, and with a high probability of coagulation, large particles are formed. Similar trends are also seen in RME fuel, where the maximum nucleation position is at 18 nm. This means that at medium and high loads, the load slightly modifies the RME nucleation mode, and the concentrations are approximately equal to the number of particles. Nucleation mode particles are emitted by RME than by ULSD, but ULSD produces more particles in accretion mode.
- The CCN values of RME in the Nuc. M were higher in most cases, while the CCN values of the Acc. M of ULSD were higher. Furthermore, all CCN values decreased with increasing IP. When changing the engine load, the size distribution of the measured particle number was in diameters from 5 to 100 nm.

According to the findings from this study, it can be concluded that the using rapeseed methyl ester as a fuel in the engine was beneficial for the environment and health issues due to the significant reduction in the size, number and concentration of soot nanoparticles and total particulate matter that emitted from the engine. Furthermore, the higher oxygen content in the RME properties enhances the oxidation of nanoparticles inside the cylinder during combustion and through the exhaust pipe as well as when move it to the environment.

Acknowledgement: A special thanks goes out to the Center for Advanced Research in Power Generation and Fuel (CAPF), Faculty of Engineering and Design, Brunel University, London, UK. It is our pleasure to extend our gratitude and appreciation to Kenneth Antiss as well as his colleagues Fanos Christodoulou and David Peirce.

Funding Statement: The authors received no specific funding for this study.

Author Contributions: The authors confirm their contribution to the paper as follows: study conception and design: Hayder A. Dhahad, Miqdam T. Chaichan; data collection: Hayder A. Dhahad; analysis and interpretation of results: Miqdam T. Chaichan, Mohammed A. Fayad, Hasanain A. Abdul Wahhab; draft manuscript preparation: Miqdam T. Chaichan and T. Magrites. All authors reviewed the results and approved the final version of the manuscript.

Availability of Data and Materials: The data that support the findings of this study are available from the corresponding author upon reasonable request.

Ethics Approval: Not applicable.

Conflicts of Interest: The authors declare no conflicts of interest to report regarding the present study.

Nomenclature

Acc.	Accumulation mode
ATDC	After top dead center
CAD	Crank angle degree
EOC	End of combustion
EOPMB	End of premixed burn
ID	Ignition delay
ULSD	Ultra-low sulfur diesel
k	The resolution of the heat release rate expressed in 1/measured points in 0.125 CAD
$\dot{m}_f$	Fuel mass flow rate
Nuc.	Nucleation mode

P	Engine output power
p	The in-cylinder pressure
PMBF	Premixed burn fraction
Qht	Convective heat transfer to the cylinder walls
SOC	Start of combustion
SOI	Start of injection
SN	Smoke Number
Us	Internal energy
V	The cylinder volume
W	Work output
γ	Adiabatic index (specific heats ratio)
θ	Crank angle degree

References

1. Bogdanov D, Ram M, Aghahosseini A, Gulagi A, Oyewo AS, Child M, et al. Low-cost renewable electricity as the key driver of the global energy transition towards sustainability. Energy. 2021;227(1):120467. doi:10.1016/j.energy.2021.120467.
2. Abed Dhahad H, Hasan AM, Chaichan MT, Kazem HA. Prognostic of diesel engine emissions and performance based on an intelligent technique for nanoparticle additives. Energy. 2022;238(1):121855. doi:10.1016/j.energy.2021.121855.
3. Abdul Wahhab HA, Al-Kayiem HH. Environmental risk mitigation by biodiesel blending from *Eichhornia crassipes*: performance and emission assessment. Sustainability. 2021;13(15):8274. doi:10.3390/su13158274.
4. Al-Kayiem HH, Wahhab HAA, Magaril E, Aziz ARA. Performance and emissions investigation of a single cylinder diesel engine using enhanced blend biodiesel by nanoparticles. In: AIP Conference Proceedings; 2018; Kuala Lumpur, Malaysia. Vol. 2035. doi:10.1063/1.5075556.
5. Nazal IT, Al-Kayiem HH. Experimental characterization of diesel engine performance fuelled by various sunflower oil-diesel mixtures. J Appl Sci. 2012;12(24):2604–9. doi:10.3923/jas.2012.2604.2609.
6. Jiaqiang E, Xu W, Ma Y, Tan D, Peng Q, Tan Y, et al. Soot formation mechanism of modern automobile engines and methods of reducing soot emissions: a review. Fuel Process Technol. 2022;235:107373. doi:10.1016/j.fuproc.2022.107373.
7. Chauhan BVS, Corada K, Young C, Smallbone KL, Wyche KP. Review on sampling methods and health impacts of fine ($PM_{2.5}$, ≤2.5 μm) and ultrafine (UFP, PM0. 1, ≤0.1 μm) particles. Atmos. 2024;15(5):572. doi:10.3390/atmos15050572.
8. Yusuf AA, Inambao FL, Ampah JD. Evaluation of biodiesel on speciated $PM_{2.5}$, organic compound, ultrafine particle and gaseous emissions from a low-speed EPA Tier II marine diesel engine coupled with DPF, DEP and SCR filter at various loads. Energy. 2022;239(13):121837. doi:10.1016/j.energy.2021.121837.
9. Nabi MN, Rahman MM, Akhter MS. Biodiesel from cotton seed oil and its effect on engine performance and exhaust emissions. Appl Therm Eng. 2009;29(11–12):2265–70. doi:10.1016/j.applthermaleng.2008.11.009.
10. Agarwal D, Sinha S, Agarwal AK. Experimental investigation of control of NO_x emissions in biodiesel-fueled compression ignition engine. Renew Energy. 2006;31(14):2356–69. doi:10.1016/j.renene.2005.12.003.
11. Ushakov S, Valland H, Æsøy V. Combustion and emissions characteristics of fish oil fuel in a heavy-duty diesel engine. Energy Convers Manag. 2013;65(10):228–38. doi:10.1016/j.enconman.2012.08.009.
12. Ekaab NS, Hamza NH, Chaichan MT. Performance and emitted pollutants assessment of diesel engine fuelled with biokerosene. Case Stud Therm Eng. 2019;13(3):100381. doi:10.1016/j.csite.2018.100381.
13. Fareed AF, El-Shafay AS, Mujtaba MA, Riaz F, Gad MS. Investigation of waste cooking and *Castor* biodiesel blends effects on diesel engine performance, emissions, and combustion characteristics. Case Stud Therm Eng. 2024;60(5):104721. doi:10.1016/j.csite.2024.104721.
14. Sharma P, Chhillar A, Said Z, Huang Z, Nguyen VN, Nguyen PQP, et al. Experimental investigations on efficiency and instability of combustion process in a diesel engine fueled with ternary blends of hydrogen peroxide

additive/biodiesel/diesel. Energy Sources Part A Recovery Util Environ Eff. 2022;44(3):5929–50. doi:10.1080/15567036.2022.2091692.
15. Viswanathan VK, Kaladgi AR, Thomai P, Ağbulut Ü, Alwetaishi M, Said Z, et al. Hybrid optimization and modelling of CI engine performance and emission characteristics of novel hybrid biodiesel blends. Renew Energy. 2022;198(4):549–67. doi:10.1016/j.renene.2022.08.008.
16. Karpanai Selvan B, Das S, Chandrasekar M, Girija R, John Vennison S, Jaya N, et al. Utilization of biodiesel blended fuel in a diesel engine-Combustion engine performance and emission characteristics study. Fuel. 2022;311(9):122621. doi:10.1016/j.fuel.2021.122621.
17. Wang D, Kuang M, Wang Z, Su X, Chen Y, Jia D. Experimental study on the impact of Miller cycle coupled EGR on a natural gas engine. Energy. 2024;294(2):130911. doi:10.1016/j.energy.2024.130911.
18. Fayad MA, Tsolakis A, Martos FJ, Bogarra M, Lefort I, Dearn KD. Investigation the effect of fuel injection strategies on combustion and morphology characteristics of PM in modern diesel engine operated with oxygenate fuel blending. Therm Sci Eng Prog. 2022;35(8–9):101476. doi:10.1016/j.tsep.2022.101476.
19. Ergen G. Comprehensive analysis of the effects of alternative fuels on diesel engine performance combustion and exhaust emissions: role of biodiesel, diethyl ether, and EGR. Therm Sci Eng Prog. 2024;47(52):102307. doi:10.1016/j.tsep.2023.102307.
20. Sujesh G, Ganesan S, Ramesh S. Effect of CeO_2 nano powder as additive in WME-TPO blend to control toxic emissions from a light-duty diesel engine—an experimental study. Fuel. 2020;278(4):118177. doi:10.1016/j.fuel.2020.118177.
21. Ge S, Pugazhendhi A, Sekar M, Xia C, Elfasakhany A, Brindhadevi K, et al. PM emissions—assessment of combustion energy transfer with *Schizochytrium* sp. algal biodiesel and blends in IC engine. Sci Total Environ. 2022;802:149750. doi:10.1016/j.scitotenv.2021.149750.
22. Karin P, Tripatara A, Wai P, Oh BS, Charoenphonphanich C, Chollacoop N, et al. Influence of ethanol-biodiesel blends on diesel engines combustion behavior and particulate matter physicochemical characteristics. Case Stud Chem Environ Eng. 2022;6(10):100249. doi:10.1016/j.cscee.2022.100249.
23. Bhangwar S, Ghoto SM, Abbasi A, Abbasi MK, Rind AA, Luhur MR, et al. Analysis of particulate matter emissions and performance of the compression ignition engine using biodiesel blended fuel. Eng Technol Appl Sci Res. 2022;12(5):9400–3. doi:10.48084/etasr.5204.
24. Al Ezzi A, Fayad MA, Al Jubori AM, Jaber AA, Alsadawi LA, Dhahad HA, et al. Influence of fuel injection pressure and RME on combustion, NO_x emissions and soot nanoparticles characteristics in common-rail HSDI diesel engine. Int J Thermofluids. 2022;15(5):100173. doi:10.1016/j.ijft.2022.100173.
25. Millo F, Vlachos T, Piano A. Physicochemical and mutagenic analysis of particulate matter emissions from an automotive diesel engine fuelled with fossil and biofuel blends. Fuel. 2021;285:119092. doi:10.1016/j.fuel.2020.119092.
26. Magno A, Mancaruso E, Vaglieco BM. Experimental investigation in an optically accessible diesel engine of a fouled piezoelectric injector. Energy. 2014;64(2):842–52. doi:10.1016/j.energy.2013.10.071.
27. Zheng F, Cho HM. The effect of different mixing proportions and different operating conditions of biodiesel blended fuel on emissions and performance of compression ignition engines. Energies. 2024;17(2):344. doi:10.3390/en17020344.
28. Agocs A, Frauscher M, Ristic A, Dörr N. Impact of soot on internal combustion engine lubrication—oil condition monitoring, tribological properties, and surface chemistry. Lubricants. 2024;12(11):401. doi:10.3390/lubricants12110401.
29. Srivastava DK, Agarwal AK, Gupta T. Particulate characterization of biodiesel fuelled compression ignition engine. SAE Technical Paper No. 2009-28-0018. SAE Organization; 2009. doi:10.4271/2009-28-0018.
30. Lapuerta M, Armas O, Ballesteros R. Diesel particulate emissions from biofuels derived from Spanish vegetable oils. SAE paper No. 2002-01-1657. SAE Organization; 2002. doi:10.4271/2002-01-1657.
31. Schneider J, Hock N, Weimer S, Borrmann S, Kirchner U, Vogt R, et al. Nucleation particles in diesel exhaust: composition inferred from in situ mass spectrometric analysis. Environ Sci Technol. 2005;39(16):6153–61. doi:10.1021/es049427m.